Lorentz Microscopy Observations of a Nanocrystalline $Fe_{44}Co_{44}Zr_7B_4Cu_1$ Alloy

Marc De Graef, Matthew A. Willard, David E. Laughlin, and Michael E. McHenry

***Abstract*—Domain imaging of soft magnetic materials by transmission electron microscopy (TEM) is difficult due to the potentially saturating field of the microscope's objective lens. Energy filtered Lorentz microscopy provides a low field, high resolution domain imaging solution for soft magnetic materials. This technique was successfully applied to a soft magnetic nanocrystalline alloy to examine the domain configurations in a thin foil sample. A sample with composition $Fe_{44}Co_{44}Zr_7B_4Cu_1$ annealed at 650 °C for one hour was examined. Both Foucault and Fresnel methods were used to develop a clear picture of the relationship between the microstructure and domain structure of this alloy. Magnetic domain maps were created showing some regions of the sample with irregularly shaped domains, which are characteristic of amorphous alloys. Other regions contained relatively large grains with the magnetization in a circular in-plane configuration (presumably due to shape anisotropy).**

***Index Terms*—Magnetic domains, nanocrystalline, phase reconstruction, soft magnetic nanocrystalline alloy.**

I. Introduction

LORENTZ microscopy is a direct technique for the observation of magnetic domain structures. It has been used during the past 4 decades in a mostly qualitative way, i.e., to *visualize* the location of domain walls and domain wall configurations; in some cases quantitative information has been derived from Lorentz images, but this is, in general, not straightforward. Recently, a new phase reconstruction method was proposed by Paganin and Nugent [1]. The method requires a through-focus series of three images from which the phase of the electron wave is reconstructed. The gradient of the phase is then proportional to the in-plane magnetization components, multiplied by the local thickness of the foil. The method can be implemented efficiently using fast Fourier transforms, as described in [2], [3]. The phase reconstruction method has been applied to Permalloy thin films [3], CoPt sputtered films, magnetization changes during the martensitic phase transformation in Ni_2MnGa alloys at low temperature [4], and in this paper we present the first results on nanocrystalline magnetic materials.

Manuscript received October 2000.

This work was supported in part by the Air Force Office of Scientific Research under Grant F49620-96-1-0454. The U.S. government is authorized to reproduce and distribute reprints for governmental purposes notwithstanding any copyright notation thereon.

M. De Graef, D. E. Laughlin, and M. E. McHenry are with the Department of Materials Science and Engineering, Carnegie Mellon University, Pittsburgh, PA, USA (e-mail: degraef@cmu.edu; dl0p@ece.cmu.edu; mm7g@andrew.cmu.edu).

M. A. Willard is with the Naval Research Laboratory, Washington DC, USA (e-mail: willard@anvil.nrl.navy.mil).

Publisher Item Identifier S 0018-9464(01)06781-4.

Nanocrystalline magnetic materials exhibit soft magnetic properties provided the grain size remains smaller than the domain wall width. According to Herzer's model [5], this condition allows averaging of local anisotropy energies for magnetization rotation and therefore domain walls will not become pinned by grain boundaries. When the grains are larger, the averaging of the anisotropic energy is lost and domain walls become pinned at grain boundaries. The presence or absence of domain wall pinning at grain boundaries in nanocrystalline materials should indicate whether or not Herzer's model is consistent with the experiment. Full characterization of a domain configuration includes determination of the size and shape of the domains, the local direction of the magnetization, and the width and character of the domain walls [6]. For this reason, induction mapping is a necessary analytical tool.

While the Lorentz force provides the classical description of the interaction of electrons with the magnetic induction of the sample, a complete description requires a quantum mechanical formalism. The deflection of an electron passing through a magnetic thin foil corresponds to an elastic momentum change which is formally equivalent to a phase change of the electron wave function. In "classical" Lorentz microscopy, the electron experiences a deflection force proportional to both the magnetic induction and the electron velocity. The deflection angle (or Lorentz angle) θ_L is given by $(e\lambda/h)B_\perp t$, with λ the relativistic electron wavelength, $B_\perp$ the magnetic induction component normal to the electron trajectory, and t the local sample thickness; θ_L is typically in the range of a few tens of microradians. The deflection of the electrons can be used in three ways to obtain images: 1) form a diffraction pattern, in which the split central beam indicates the magnetization directions present in the sample; 2) insert an aperture in the back focal plane to select one of the components of the split central beam (*Foucault mode*); 3) defocus the image, so that electrons scattered in different directions may overlap and produce bright contrast at domain wall locations (*Fresnel mode*). Of these methods, only the first is quantitative, since the deflection angle may be directly measured from the diffraction pattern. Foucault images are easy to obtain, but it is difficult to mechanically position the aperture in a reproducible way. Fresnel images are by nature somewhat fuzzy, and only show the location of domain walls; they typically do not provide any information about the nature of the wall.

Lorentz TEM observations require that the sample be mounted in a low-field or field-free region of the microscope column, so that the lens field (in the range 1–2 T) will not saturate the magnetization of the sample. As a consequence Lorentz images are typically obtained at a low magnification, in the

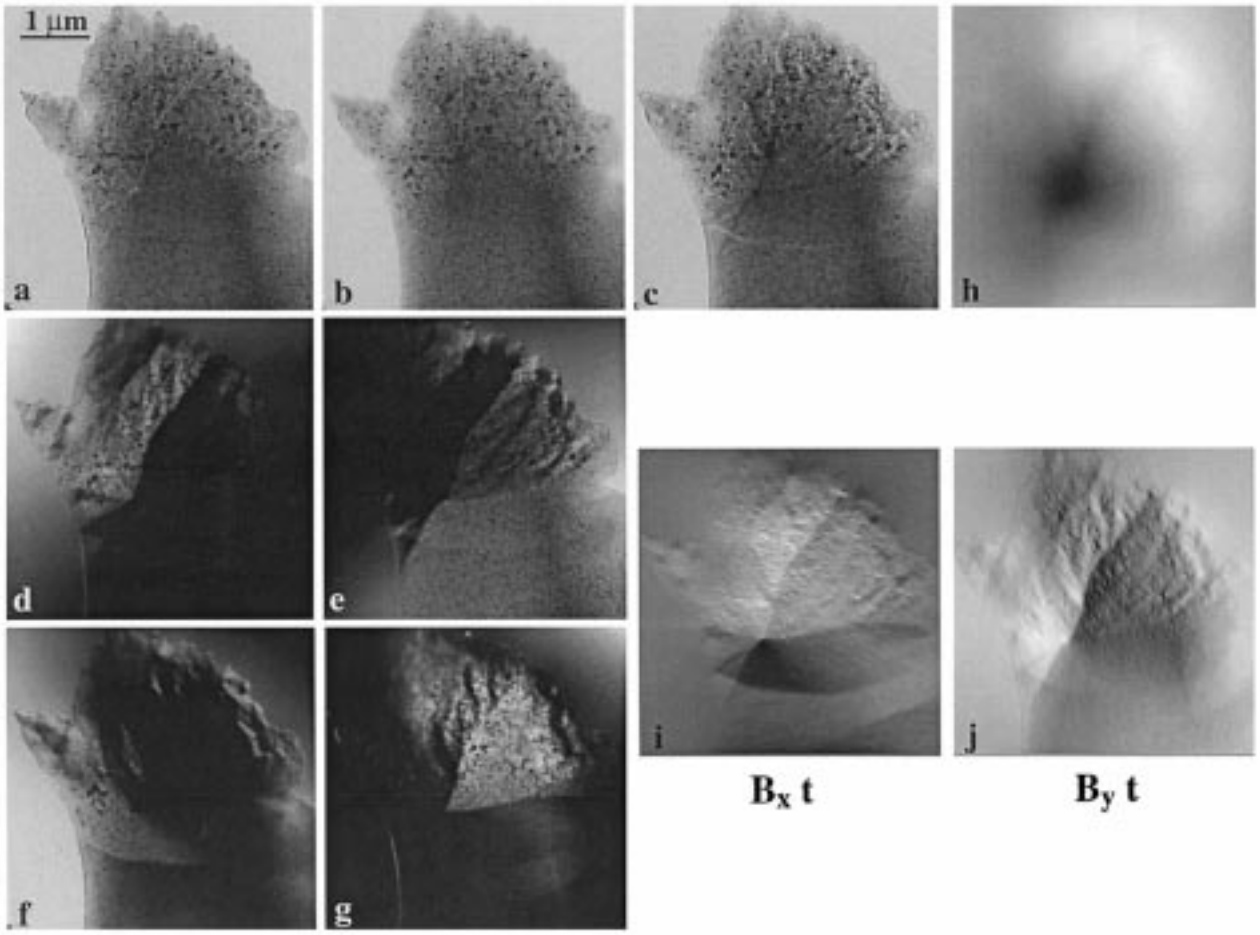

Fig. 1. Lorentz images of a $Fe_{44}Co_{44}Zr_7B_4Cu_1$ ribbon sample annealed at 650 °C for 1 hour. (a)–(c) Under-focus, in-focus, over-focus; (d)–(g) Foucault images for four different orthogonal aperture shifts; (h) reconstructed phase map; (i) and (j) $B_x t$ and $B_y t$ magnetic induction maps (bright indicates a positive component).

range 400–3000×. It is possible to increase the magnification range if a post-column energy filter (Gatan Imaging Filter or GIF) is used; the GIF has an internal magnification of around 20×, and acquires images on a 1K × 1K CCD camera, so that the final magnification is more than 100 000×. Details of the use of an energy filter for Lorentz microscopy are described by Dooley and De Graef [7].

The phase of the electron wave scattered by a magnetic thin foil may be reconstructed from a set of two Fresnel images and the in-focus image. The details of this method may be found elsewhere [3]. In short, the algorithm first aligns all three images with respect to a common origin, then subtracts the over-focus image from the under-focus image, to obtain the derivative of intensity along the beam direction. From this derivative the algorithm reconstructs the phase, using a formal solution to the so-called *Transport-of-Intensity* equation, or TIE [1]. The reconstructed phase profile is qualitatively correct, and if microscope magnification and defocus have been calibrated, the algorithm has the potential to accurately and quantitatively provide the phase and hence the magnetic induction (which is proportional to the gradient of the phase).

II. Experimental Methods and Observations

The sample used for Lorentz observations had a composition of $Fe_{44}Co_{44}Zr_7B_4Cu_1$, and was annealed at 650 °C for one hour. Thin foils were prepared by precision ion polishing (PIPS). Special care was taken to preserve the demagnetized domain structure. A JEOL 4000EX 400 kV high-resolution transmission electron microscope was used to examine the thin foils. The objective lens was turned off and a post-column GIF was used to remove inelastically scattered electrons and acquire digital images.

Fresnel and Foucault images were recorded for a nanocrystalline region of the specimen as seen in Fig. 1. Fig. 1(a)–(c) are Fresnel or out-of-focus images, Fig. 1(d)–(g) are Foucault images for four different aperture shifts (along orthogonal directions). The salt-and-pepper contrast of the sample indicates the size of the nanocrystallites. The domain shape is similar to that found in amorphous alloys and Fe-based nanocrystalline alloys [8]. The domains are significantly larger than the nanocrystalline grains and the domain walls do not seem to follow the nanocrystals. This is consistent with the Herzer model. Several domain walls can be observed; they intersect at a point to the left of the center of the images. Fig. 1(h) is the reconstructed phase map; the intersection of domain walls corresponds to a nearly conical depression in the phase (dark region). The gradient of the phase is proportional to the in-plane magnetic induction component multiplied by the local sample thickness. The induction components are shown as grayscale images in Fig. 1(i) and (j). Bright regions have a positive vector component, dark regions a negative component.

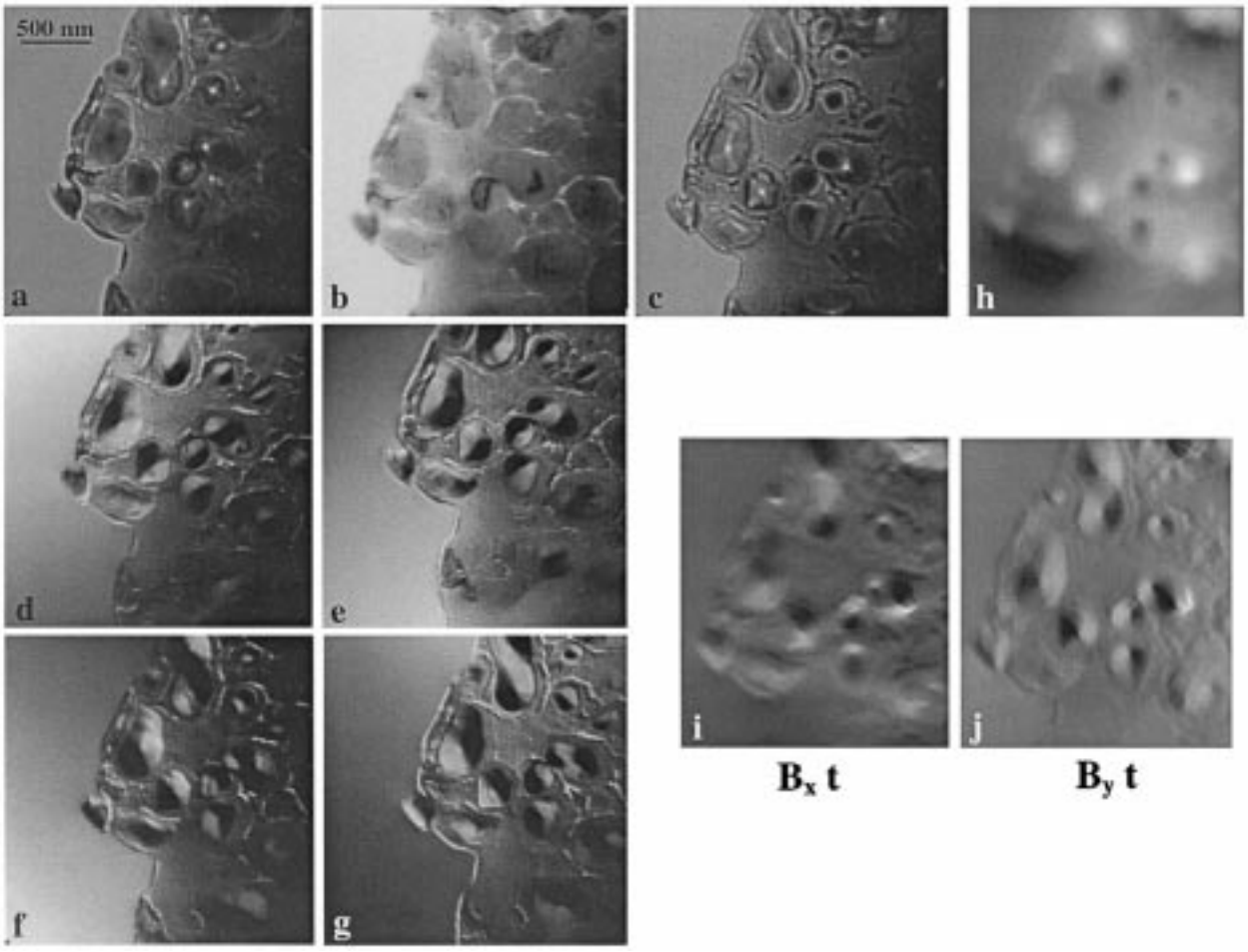

Fig. 2. Set of Lorentz images of a region in a $Fe_{44}Co_{44}Zr_7B_4Cu_1$ ribbon sample annealed at 650 °C for 1 hour. Same legend as in Fig. 1.

Fig. 2 shows a microcrystalline region of the specimen, close to the ribbon surface, where the crystallization conditions are somewhat different from those in the bulk of the foil. Again, Fresnel images [Fig. 2(a) and (c)] and Foucault images [Fig. 2(d)–(g)] reveal the domain structure. The reconstructed phase indicates the presence of closure domains in each of the larger round grains. Bright regions correspond to domains with a counterclockwise closure pattern, whereas dark regions in the phase image have the opposite rotation. The in-plane magnetic induction components are shown in Fig. 2(i) and (j), and are consistent with this interpretation. The closure domains are most likely due to shape anisotropy of the larger particles (they are disc-shaped, with the disc normal along the foil normal and the beam direction), which causes most of the magnetic induction to lie in the plane of the foil.

Magnetic force microscopy [9] and conversion electron Mössbauer spectroscopy [10] indicate that the ribbon surface is indeed quite different from that of the ribbon interior. Additional information supporting the differences between the bulk and surfaces of the ribbons are also observed by Scherrer analysis of X-ray diffraction with bright field/dark field analysis of transmission electron micrographs [11].

III. Conclusions

Differences between the bulk (nanocrystalline) and surface (microcrystalline) regions of the FeCo-based alloy were observed in both the microstructure and magnetic domain structure. Nanocrystalline regions exhibited domain structures with no discernible pinning of the domain wall on the grain boundaries, in agreement with the Herzer model. Microcrystalline regions showed closure domains consisting of single grains.

References

[1] D. Paganin and K. Nugent, "Noninterferometric phase imaging with partially coherent light," *Phys. Rev. Lett.*, vol. 80, pp. 2586–2589, 1998.

[2] A. Barty, D. Paganin, and K. A. Nugent, "Phase retrieval in Lorentz microscopy," in *Magnetic Microscopy and its Applications to Magnetic Materials*, M. De Graef and Y. Zhu, Eds: Academic Press, 2000, vol. 36, Experimental Methods in the Physical Sciences.

[3] M. De Graef and Y. Zhu, "Quantitative noninterferometric Lorentz microscopy," J. Appl. Phys., 2000, submitted for publication.

[4] M. De Graef, M. Willard, M. E. McHenry, and Y. Zhu, "*In-situ* Lorentz TEM cooling study of magnetic domain configurations in Ni_2MnGa," IEEE Trans. Magn., 2000, submitted for publication.

[5] G. Herzer, "Grain size dependence of coercivity and permeability in nanocrystalline ferromagnets," *IEEE Trans. Magn.*, vol. 26, pp. 1397–1402, 1990.

[6] M. De Graef, *Introduction to Conventional Transmission Electron Microscopy*: Under contract with Cambridge University Press, 1999.

[7] J. Dooley and M. De Graef, "Energy filtered Lorentz microscopy," *Ultramicroscopy*, vol. 67, pp. 113–131, 1997.

[8] R. Schäfer, A. Hubert, and G. Herzer, "Domain observation on nanocrystalline material," *J. Appl. Phys.*, vol. 69, pp. 5325–5328, 1991.

[9] M. E. Hawley, G. W. Brown, D. J. Thoma, M. A. Willard, D. E. Laughlin, and M. E. McHenry, "Magnetic force microscopy study of new nanocrystalline soft magnetic ribbons," in *MRS Symp. Proc.*, vol. 577, 1999, pp. 531–542.

[10] M. Kopcewicz, A. Grabias, M. A. Willard, D. E. Laughlin, and M. E. McHenry, "Mössbauer measurements for a nanocrystalline alloy," IEEE Trans. Mag., 2000, submitted for publication.

[11] M. A. Willard, "Structural and magnetic characterization of HITPERM soft magnetic materials for high temperature applications," Ph.D. thesis, Carnegie Mellon University, 2000.

[12] M. A. Willard, D. E. Laughlin, M. E. McHenry, D. Thoma, K. Sickafus, J. O. Cross, and V. G. Harris, "Structure and magnetic properties of $(Fe_{0.5}Co_{0.5})_{88}Zr_7B_4Cu_1$ nanocrystalline alloys," *J. Appl. Phys.*, vol. 84, pp. 6773–6777, 1998.